Journal of Intelligent & Robotic Systems
https://doi.org/10.1007/s10846-018-0895-4

Simultaneous Merging Multiple Grid Maps Using the Robust Motion Averaging

Zutao Jiang[1] · Jihua Zhu[1] · Yaochen Li[1] · Jun Wang[2] · Zhongyu Li[3] · Huimin Lu[4]

Received: 19 July 2017 / Accepted: 21 June 2018

Abstract

Mapping in the GPS-denied environment is an important and challenging task in the field of robotics. In the large environment, mapping can be significantly accelerated by multiple robots exploring different parts of the environment. Accordingly, a key problem is how to integrate these local maps built by different robots into a single global map. In this paper, we propose an approach for simultaneous merging of multiple grid maps by the robust motion averaging. The main idea of this approach is to recover all global motions for map merging from a set of relative motions. Therefore, it firstly adopts the pair-wise map merging method to estimate relative motions for grid map pairs. To obtain as many reliable relative motions as possible, a graph-based sampling scheme is utilized to efficiently remove unreliable relative motions obtained from the pair-wise map merging. Subsequently, the accurate global motions can be recovered from the set of reliable relative motions by the motion averaging. Experimental results carried on real robot data sets demonstrate that the proposed approach can achieve simultaneous merging of multiple grid maps with good performances.

Keywords Multi-robot systems · Grid map merging · Iterative closet point · Image registration · Motion averaging

1 Introduction

Mapping is one of the most fundamental issues in robotics, and has attracted much attention since the seminal work presented in [1]. In the past few decades, many simultaneous localization and mapping(SLAM) approaches have been proposed to build different environment maps, such as topological map [2, 3], grid map [4, 5], and feature map [6] etc. As the occupancy grid map is not required to extract any special features from environments, it can easily model arbitrary types of environments. Therefore, the grid map is one of the most popular map representations in robot mapping. However, most of robot mapping approaches can only build single map for medium scale environments. For the large scale environment, multi-robots should cooperatively explore various parts of the same environment so as to build grid map with good efficiency and accuracy. Accordingly, multi-robot SLAM algorithms were proposed to build large grid maps [5–8]. Although these approaches can build large map, the memory requirement is large for carrying the individual map of the large environment. Besides, the communication should be kept between multi-robot during mapping.

Different from the multi-robot SLAM algorithm, another feasible method is to build local grid maps by different robots and integrate them into a single global map. To merge grid map pair, Carpin et al. viewed it as the optimization problem [9], where the optimal transformation should be searched to align two grid maps. Subsequently, two stochastic search approaches were proposed to solve this optimization problem [9, 10]. Similarly, Li et al. proposed a grid map merging approach based on the genetic algorithm [11]. Although these approaches may obtain the optimal rigid transformation, they are all time-consuming due to

Electronic supplementary material The online version of this article (https://doi.org/10.1007/s10846-018-0895-4) contains supplementary material, which is available to authorized users.

✉ Jihua Zhu
zhujh@xjtu.edu.cn

[1] School of Software Engineering, Xi'an Jiaotong University, Xi'an, People's Republic of China

[2] School of Digital Media, Jiangnan University, Wuxi, People's Republic of China

[3] Department of Computer Science, University of North Carolina at Charlotte, Charlotte, NC, USA

[4] Kyushu Institute of Technology, Kitakyushu, Japan

Published online: 03 August 2018

the nature of exhaustive search. What's more, Carpin et al. then proposed map merging approach based on the Hough transform [12], which can merge grid maps containing the line features. Although this approach can efficiently merge grid map without any line feature extraction, its accuracy should be further improved due to the nature of discretization error in the Hough transform. Besides, it is required that the potentially being merged grid maps should contain a significant overlapping percentage. To address the accuracy issue, Zhu et al. [13] viewed the grid map merging as the point set registration problem and accomplished it by the trimmed iterative closest point (TrICP) [14, 15], where the initial parameters are provided by the Hough transform. Meanwhile, Blanco et al. [16] proposed a multi-hypothesis method to provide the initial parameters for point set registration algorithm so as to merge grid maps. By the confirmation of merging hypotheses, it can obtain the robust merging result. To address the robustness issue, Saeedi et al. [17] proposed the improved grid map merging approach based on the Hough transform, which can merge grid map pair even with low overlapping percentage. To merge grid maps with different resolutions, Ma et al. [18] put forward an image registration based approach, which can determine whether one of the two maps should be magnified in order to be merged with the other. Although many approaches can merge grid map pair with good performances, few of them can simultaneously merge multiple grid maps.

Suppose there is a set of grid maps, which were built by multiple robots exploring different parts of the same environment. Given the reference map, the goal of map merging is to integrate these local maps into a global map by calculating the global motion for each grid map. To solve this problem, the pair-wise merging algorithm can repeatedly merge two grid maps and integrate them into one until all the maps are integrated together. However, this kind of approach suffers from the error accumulative problem. As mentioned in [13, 18], the problem of pair-wise grid map merging can be viewed as the pair-wise registration problem [19]. Accordingly, the problem of multiple grid map merging can also be viewed as multi-view registration problem [20–25]. However, most of multi-view registration should be provided with the good initial motions in advance [21–24]. Otherwise, they are unable to accomplish the multi-view registration. Besides, although some existing approaches can achieve multi-view registration without initial motions, they are designed to deal with 3D range scan and always time-consuming [20]. Therefore, it is required to design an automatic multi-view registration approach, which can efficiently deal with 2D grid maps. Recently, motion averaging algorithm has been introduced as an effective means to solve the multi-view registration problem [26]. To accomplish the multi-view registration, it should be provided with initial global motions and reliable pair-wise registration results [22, 27].

This paper proposes an effective map merging approach, which can simultaneously merge multiple grid maps without any prior information. The main contributions are listed as follows: (1) The pair-wise merging method is presented to estimate the relative motion and its reliability. (2) Given a set of relative motions, the optimal maximal connected subgraph (MCS) sampling and confirming strategy is proposed to estimate initial global motions and confirm all reliable relative motions. (3) Given initial global motions, the 2D motion averaging algorithm is presented to deal with all relative motions so as to obtain accurate global motions.

This paper is organized as follows. In the next section, the grid map merging problem is stated and the TrICP algorithm is briefly reviewed. Section 3 proposes our map merging approach. In Section 4, the proposed approach is tested on robot data sets. Finally, conclusions are drawn in Section 5.

2 Problem Statement and the TrICP algorithm

This section states the problem of grid map merging and then briefly reviews the 2D TrICP algorithm for the pair-wise map merging.

2.1 Problem Statement

To build large grid map, mapping can be cooperatively implemented by multiple robots exploring different parts of the environment. Accordingly, a set of local grid maps built by different robots should be integrated into one global grid map.

Suppose there are two local grid maps built by robots exploring two parts of the same environment. According to [12], the goal of pair-wise map merging is to find a relative motion:

$$\mathbf{M} = \begin{bmatrix} \mathbf{R} & t \\ 0 & 1 \end{bmatrix}, \tag{1}$$

with which these two local maps can be properly integrated into a global map. More specifically, $\mathbf{R} \in \mathbb{R}^{2\times 2}$ denotes a

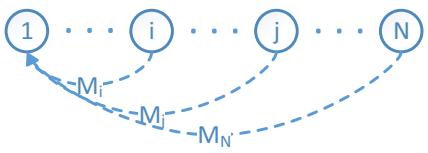

Fig. 1 The diagram of multiple grid map merging, where one circle represents a grid map and dashed curves indicate global motions required to be estimated

rotation matrix determined by the angle θ and $t \in \mathbb{R}^2$ is a translation vector:

$$\mathbf{R} = \begin{bmatrix} \cos\theta & -\sin\theta \\ \sin\theta & \cos\theta \end{bmatrix}, \quad t = \begin{bmatrix} t_x \\ t_y \end{bmatrix}. \tag{2}$$

Given a set of local grid maps, the merging of multiple maps is to integrate them into a single global map. Without loss of generality, the first map can be viewed as the reference map. Therefore, as shown in Fig. 1, this problem is equivalent to obtain a set of global motions $\mathbf{M}_{global} = \{\mathbf{I}, \mathbf{M}_2, ..., \mathbf{M}_N\}$, so that these local maps can be properly integrated into one global map.

2.2 The TrICP Algorithm

Suppose there are two grid maps with overlapping areas, the model map P and the subject map Q, where ξ represents their overlapping percentage. By applying the edge extraction algorithm, two edge point sets $P \triangleq \{p_i\}_{i=1}^{N_p}$ and $Q \triangleq \{q_j\}_{j=1}^{N_q}$ can be extracted from these two grid maps to be merged. Denote P_ξ as the point subset, which corresponds the overlapping part of the subject map to the model map. For pair-wise map merging, the relative motion $\mathbf{M}$ can be estimated by minimizing the following objective function:

$$\begin{aligned} &\arg\min_{\xi,\mathbf{R},t} \frac{\sum_{p_i \in P_\xi} \|\mathbf{R}p_i + t - q_{c(i)}\|_2^2}{|P_\xi|\xi^{1+\lambda}} \\ &\text{s.t.} \quad \mathbf{R}^{\mathrm{T}}\mathbf{R} = \mathrm{I}_2, \det(\mathbf{R}) = 1 \end{aligned} \tag{3}$$

where I_2 denotes the 2D identity matrix and λ is a preset parameter.

Actually, Eq. 3 can be solved by the TrICP algorithm [14, 15], which can obtain the optimal relative motion by iterations. Given the initial relative motion $\mathbf{M}_0$, three steps are included in each iteration of this algorithm:

(1) Based on the previous motion, establish the point correspondence for each edge point in the subject map:

$$c_k(i) = \arg\min_{j \in \{1,2,\cdots,N_q\}} \left\|\mathbf{R}_{k-1}p_i + t_i - q_j\right\|_2 \qquad i = 1, 2, \cdots N_p. \tag{4}$$

(2) Update the kth overlapping percentage and its corresponding subset:

$$(\xi_k, P_{\xi_k}) = \arg\min_{\xi} \sum_{p_i \in P_\xi} \left\|\mathbf{R}_{k-1}p_i + t_{k-1} - q_{c_k(i)}\right\|_2^2 / (|P_\xi|(\xi)^{1+\lambda}) \tag{5}$$

(3) Calculate the current relative motion:

$$\mathbf{M}_k \triangleq (\mathbf{R}_k, t_k) = \arg\min_{\mathbf{R},t} \sum_{p_i \in P_{\xi_k}} \left\|\mathbf{R}p_i + t - q_{c(i)}\right\|_2^2 \tag{6}$$

Finally, the optimal relative motion can be obtained by repeating these three steps until some stop conditions are satisfied. It should be noted that the TrICP algorithm can only obtain reliable relative motions for the grid map pair, which contains a certain amount of overlapping percentage [28].

3 Merging Multiple Grid Maps

This section proposes the effective approach for simultaneous merging of multiple grid maps by the robust motion averaging.

Given a set of gird maps, the proposed approach can accomplish grid map merging by three steps displayed in Fig. 2. Firstly, the pair-wise merging method is presented to estimate the relative motions for many grid map pairs. Subsequently, all grid maps and the estimated relative motions can be viewed as an undirected graph, where each vertex denotes a grid map and each edge indicates an estimated relative motion between the two vertices. Then, a randomized sampling scheme is utilized to find the MCS. As there may exist unreliable relative motions obtained from

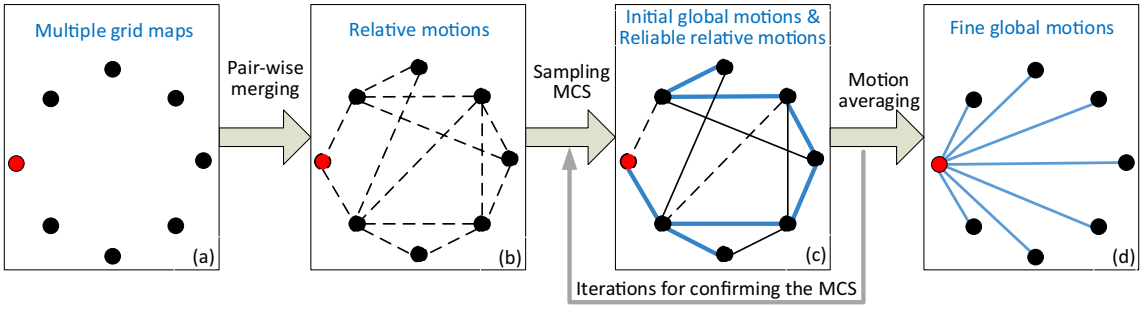

Fig. 2 The flowchart of our approach, where each vertex denotes a grid map, each edge indicates the relative motion of connected vertexes. **a** Multiple grid maps to be merged, where the red one is the reference map. **b** A set of relative motions obtained by the pair-wise merging. **c** The confirmed MCS is connected by thick lines, which denote all reliable relative motions along with other solid lines. **d** The accurate global motions denoted by thick lines

the pair-wise merging step, the sampling MCS should be confirmed by all relative motions. The process of MCS sampling and confirming should be repeated until the preset number of iteration reaches so as to search for the optimal MCS and eliminate unreliable relative motions. Finally, the accurate global motions can be recovered by the application of the 2D motion averaging algorithm to all reliable relative motions.

3.1 Pair-Wise Grid Map Merging

To estimate the relative motion $\mathbf{M}_{ij}$, the pair-wise grid map merging method should be well designed. As mentioned before, the TrICP algorithm can be utilized to estimate the relative motion of one map pair which includes a certain amount of overlapping percentage. However, owing to the local convergence property, good initial relative motion should be provided to the TrICP algorithm. Otherwise, it is easy to be trapped into the local minimum and obtain the unreliable relative motion.

For the pair-wise map merging, the scale-invariant feature transform (SIFT) features [29, 30] can be extracted from the grid map pair. As the SIFT features are invariant to rotation and translation changes, it is easy to establish feature matches between these two grid maps. Due to the sensor noise and the accuracy of mapping algorithm, there might exist some false matches. As shown in Fig. 3, there are two grid maps P and Q, which include overlapping areas. Suppose there are a set of SIFT feature matches $\{F_{i,P}, F_{i,Q}\}_{i=1}^{N}$ between two grid maps. Obviously, if the match $\{F_{i,P}, F_{i,Q}\}$ is true, the SIFT features $F_{i,P}$ and $F_{i,Q}$ must correspond to the same location of the environment, and they should satisfy the following equation:

$$\left\|\mathbf{R} f_{i,P} + t - f_{i,Q}\right\|_2^2 \approx 0, \tag{7}$$

where $\mathbf{M} \triangleq (\mathbf{R}, t)$ denotes the relative motion of these two grid maps, $f_{i,P}$ and $f_{i,Q}$ represent the locations of SIFT features $F_{i,P}$ and $F_{i,Q}$, respectively. However, the false feature match does not meet this requirement.

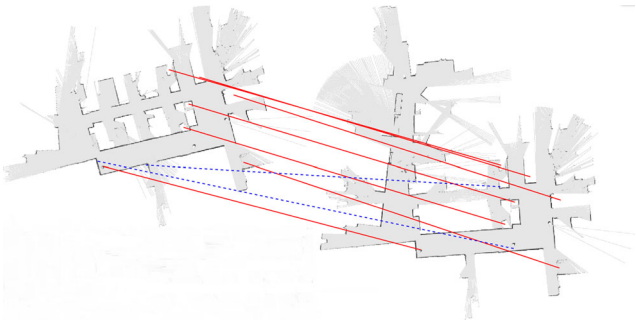

Fig. 3 SIFT features extracted and matched from grid map pair, where solid lines denote the true matches and dash lines indicate the false matches

According to Eq. 6, two true feature matches are enough to estimate the initial relative motion for the TrICP algorithm. Therefore, the random sample consensus (RANSAC) algorithm can be used to find the true matches. More specifically, two feature matches can be randomly selected from all feature matches so as to calculate the guess of relative motion $\tilde{\mathbf{M}}$, then Eq. 7 can be used to test all established feature matches and count the number of true feature matches. And the best guess $\tilde{\mathbf{M}}_{best}$ corresponds to the one, which can receive the support of all true matches. To obtain the best guess, the random guess should be repeatedly generated and tested until the preset maximum number of iteration reaches. Finally, the best guess $\tilde{\mathbf{M}}_{best}$ can be viewed as the initial relative motion of the TrICP algorithm so as to refine the relative motion of two grid maps to be merged.

Based on the above description, the proposed pair-wise map merging method can be summarized as the Algorithm 1.

Algorithm 1 Pair-wise grid map merging algorithm

Input: Grid maps P and Q
Output: The relative motion $\hat{\mathbf{M}}$ and the trimmed MSE
Extract SIFT features for P and Q, respectively;
Establish all the feature matches $\{F_{i,P}, F_{i,Q}\}_{i=1}^{N}$ and set $k = 0$;
Do
$k = k + 1$;
Randomly select two matches $\{F_{i,P}, F_{i,Q}\}_{i=m,n}$;
Calculate the motion guess $\tilde{\mathbf{M}}_k$ by Eq.(6);
Compute $d_i = \left\|\mathbf{R} f_{i,P} + t - f_{i,Q}\right\|_2$ for each feature match;
Count the number N_k of feature matches with $d_i \leq d_{thr}$;
If $N_k > N_{best}$
$N_{best} = N_k$;
$\tilde{\mathbf{M}}_{best} = \tilde{\mathbf{M}}_k$;
End
While $(k < 200)$
Extract the edge point sets $P \triangleq \{p_i\}_{i=1}^{N_p}$ and $Q \triangleq \{q_j\}_{j=1}^{N_q}$;
Obtain $\hat{\mathbf{M}}$ and MSE by refining $\tilde{\mathbf{M}}_{best}$ with the TrICP algorithm.

Theoretically, two true feature matches are enough to estimate the initial relative motion for the TrICP algorithm. However, if the number of true matches is less than three, there is no way to confirm and calculate the correct initial motion. To guarantee the robustness, the TrICP algorithm is only applied to these map pairs, which satisfy $\tilde{\mathbf{M}}_{best} \geq 4$.

Otherwise, there is no need to apply the TrICP algorithm. Suppose SIFT features has been extracted for grid maps P and Q. To establish the feature matches, we can either search the nearest neighbor from the map Q for each SIFT feature in the map P or vice verse. In practice, these two strategies can obtain different number of consistent matches for these two grid maps to be merged. Therefore, during the establishment of feature matches, both strategies should be implemented so as to obtain as many consistent matches as possible. Besides, the trimmed mean squared error (MSE) can be calculated from Eq. 6. As all edge point sets are directly extracted from the grid maps, so the resolutions of edge points for each grid maps are almost similar. Accordingly, the smaller the trimmed MSE is, the more accurate result the pair-wise map merging is. Hence, the trimmed MSE can be used to evaluate the accuracy and reliable of pair-wise grid map merging results.

After the pair-wise map merging, a set of relative motions can be obtained for the graph construction so as to sample and confirm the optimal MCS.

3.2 MCS Sampling and Confirming

Among these estimated relative motions, there may exist some unreliable relative motions due to the unreasonable application of the pair-wise merging method to these grid map pairs, which contain low percentage or even non-overlapping. Therefore, the optimal MCS should be confirmed so as to calculate initial global motions and eliminate unreliable relative motions for the motion averaging.

Given a set of relative motions $\{\hat{\mathbf{M}}_{ij}^{r}, MSE^{r}\}_{r=1}^{R}$, it is easy to construct an undirected and weighted graph G, where one vertex denotes a grid map and each edge indicates the estimated relative motion of its connected grid maps. Besides, each edge can be assigned a weight $w_{ij} = 1/MSE_{ij}$ to indicate the reliable of each relative motion. From the weighted graph G, the reasonable approach can be utilized to randomly sample the MCS, which is composed of $(N-1)$ edges and N vertexes of the graph G. As displayed in Fig. 4, based on the MCS, the global motion guess of the ith grid map can be directly set as $\tilde{\mathbf{M}}_i = \hat{\mathbf{M}}_{1i}$, where $\hat{\mathbf{M}}_{1i}$ has been estimated by the pair-wise map merging. Subsequently, the global motion of the jth grid map can be calculated as:

$$\tilde{\mathbf{M}}_j = \tilde{\mathbf{M}}_i \, \hat{\mathbf{M}}_{ij}. \tag{8}$$

where $\hat{\mathbf{M}}_{ij}$ has been estimated and included in the relative motion set $\{\hat{\mathbf{M}}_{ij}^{r}\}_{r=1}^{R}$. As the MCS exits a path between the 1st vertex to all other vertexes in the G, Eq. 8 can be transitively used to calculate all other global motions. The main questions arising here are how to sample the MCS from the graph G and how to confirm the optimal MCS.

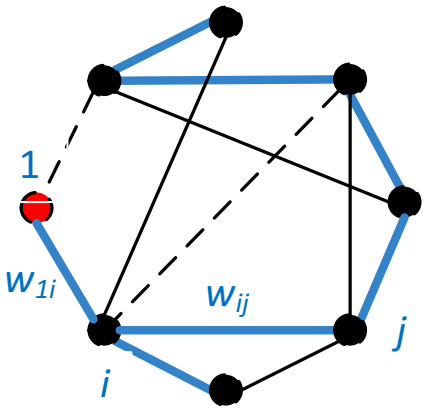

Fig. 4 Diagram of the sampled MCS, which is connected by thick lines. Each dashed line denotes one unreliable relative motion

To sample a random MCS, we can set a null matrix $\mathbf{L}$ of the size $N \times N$. As one MCS contains $(N-1)$ edges of the graph G, a subgraph G' with all vertex of G can be generated by selection of $(N-1)$ relative motions from the motion set $\{\hat{\mathbf{M}}_{ij}^{r}\}_{r=1}^{R}$. In order to select the desired MCS efficiently, $(N-1)$ edges can be sampled from the edge set $\{\hat{\mathbf{M}}_{ij}^{r}\}_{r=1}^{R}$ with the probability proportional to their importance weight. Then we can set $\mathbf{L}(i,j) = 1$, if the corresponding relative motion $\hat{\mathbf{M}}_{ij}^{r}$ is included in the subgraph G'. Subsequently, a matrix $\mathbf{g}$ can be calculated as follows:

$$\mathbf{g} = (\mathbf{L} + \mathbf{L}' + \mathbf{I}_N)^N \tag{9}$$

where $\mathbf{I}_N$ denotes the identity matrix of the size $N \times N$. If and only if all the elements of the matrix $\mathbf{g}$ are non-zeros, the subgraph G' can be viewed as a MCS of the graph G.

As displayed in Fig. 4, only $(N-1)$ relative motions are contained in the sampled MCS. Hence, all other relative motions can be used to confirm the sampled MCS. Because each edge of the optimal MCS corresponds to a reliable relative motion, Eq. 8 can be transitively used to calculated all global motions $\tilde{\mathbf{M}}_{global} = \left\{\mathbf{I}, \tilde{\mathbf{M}}_2, ..., \tilde{\mathbf{M}}_m, ..., \tilde{\mathbf{M}}_n, \tilde{\mathbf{M}}_N\right\}$ with good accuracy. Suppose the graph G includes an reliable relative motion $\hat{\mathbf{M}}_{mn}$, which is not contained in the optimal MCS. Since the relative motion $\hat{\mathbf{M}}_{mn}$ estimated by the pair-wise merging algorithm, it inevitably contains error. Therefore,

$$\hat{\mathbf{M}}_{mn} \approx \tilde{\mathbf{M}}_m^{-1} \, \tilde{\mathbf{M}}_n. \tag{10}$$

However, this relationship no longer holds for the unreliable relative motions. In practice, Eq. 10 can be replaced by the following constraint:

$$d(\hat{\mathbf{M}}_{ij}, \tilde{\mathbf{M}}_i^{-1} \tilde{\mathbf{M}}_j) = \left\| \hat{\mathbf{M}}_{ij} - \tilde{\mathbf{M}}_i^{-1} \tilde{\mathbf{M}}_j \right\|_F \leq d_{thr} \tag{11}$$

where d_{thr} denotes the preset distance threshold. Based on this constraint, all estimated relative motions can be used to

confirm the optimal MCS, which can receive the support of most relative motions in the graph.

The randomly sampled MCS is not necessary optimal due to the existence of unreliable relative motions, so the sampling and confirming of MCS should be repeatedly until the preset maximum number of iterations are reached. Accordingly, the proposed MCS sampling and confirming method can be summarized as the Algorithm 2.

Algorithm 2 MCS sampling and confirming

Input: All the weighted relative motions $\{\hat{\mathbf{M}}_{ij}^{r}, {w_{ij}}^{r}\}_{r}^{R}$

Output: Global motions $\hat{\mathbf{M}}_{global}$ and reliable relative motions $\{\hat{\mathbf{M}}_{ij}^{r}\}_{r}^{R'}$

$E_{best} = 0$ and $k = 0$;
Construct the weighted graph $\mathbf{G}$ based on $\{\hat{\mathbf{M}}_{ij}^{r}, {w_{ij}}^{r}\}_{r}^{R}$;
If $(k \leq N^2)$
  $k = k + 1$;
  do
    Sample the subgraph $\mathbf{G}'$ from the weighted graph G;
    Compute the matrix $\mathbf{g}$ denoted by Eq. 9;
  Until (All elements of $\mathbf{g}$ are non-zeros)
  Estimate $\tilde{\mathbf{M}}_{global}^{r}$ from the MCS by Eq. 8;
  Count the number E_r of edges that satisfy $d(\hat{\mathbf{M}}_{ij}, \tilde{\mathbf{M}}_{i}^{-1}\tilde{\mathbf{M}}_{j}) \leq d_{thr}$;
  If $(E_r \geq E_{best})$
    $\hat{\mathbf{M}}_{global} = \tilde{\mathbf{M}}_{global}^{r}$
    Eliminate edges from $\{\hat{\mathbf{M}}_{ij}^{r}\}_{r}^{R}$, which satisfy $d(\hat{\mathbf{M}}_{ij}, \tilde{\mathbf{M}}_{i}^{-1}\tilde{\mathbf{M}}_{j}) > d_{thr}$;
  end
end

After the MCS sampling and confirming, the initial global motions and all reliable relative motions can be obtained for the motion averaging.

3.3 Motion Averaging

Although global motions have been estimated from the optimal MCS by transitively using Eq. 8, they are coarse due to the accumulative error. Since a set of reliable relative motions have been confirmed by the optimal MCS, they can be incorporated to optimize the coarse global motions. The key question arising here is how to use these 2D relative motions so as to refine the coarse global motions. In [26], Govindu et al. proposed the 3D motion averaging algorithm, which can refine the coarse global motions by a set of relative motions. For the 2D motion, the original motion averaging algorithm should be extended.

In fact, the 2D motion $\mathbf{M} \in SE(2)$ belongs to the Lie group and its logarithm belongs to the Lie algebra $\mathbf{m} \in SE(2)$, which can be denoted as follows:

$$\mathbf{m} = \mathrm{logm}(\mathbf{M}) = \begin{bmatrix} \Omega & u \\ 0 & 0 \end{bmatrix}, \tag{12}$$

where $u = [u_1, u_2]^T$ is a vector and Ω is a skew-symmetric matrix:

$$\Omega = \begin{bmatrix} 1 & \Omega_{12} \\ -\Omega_{12} & 1 \end{bmatrix}. \tag{13}$$

Accordingly, the Lie algebra $\mathbf{m} \in SE(2)$ can be transformed into other form $v = vec(\mathbf{m})$, where $vec(.)$ indicates the function which can arrange all parameters of $\mathbf{m}$ into a compated 3D column vector. Vice verse, $rvec(.)$ can be utilized to denote the inverse function of $vec(.)$. By applying the first-order approximation to the Riemannian distance [26], there exists the following relationship for two approximate motions $\mathbf{M}_i$ and $\mathbf{M}_j$:

$$\begin{aligned} &\mathrm{logm}(\mathbf{M_i}^{-1}\mathbf{M}_j) \approx \mathrm{logm}(\mathbf{M}_i) - \mathrm{logm}(\mathbf{M}_j) \\ &\Rightarrow \mathbf{m}_{ij} \simeq \mathbf{m}_i \text{ - } \mathbf{m}_j, \end{aligned} \tag{14}$$

where the more these two motions are approximate, the more $\mathbf{m}_{ij}$ approximates to the term $(\mathbf{m}_i \text{ - } \mathbf{m}_j)$.

Algorithm 3 Global motion refining

Input: Initial global motions $\hat{\mathbf{M}}_{global} = \{\mathrm{I}, \hat{\mathbf{M}}_2, \cdots, \hat{\mathbf{M}}_N\}$
  reliable relative motions $\{\hat{\mathbf{M}}_{ij}^{r}\}_{r=1}^{R'}$

Output: Fine global motions $\mathbf{M}_{global} = \{\mathrm{I}, \mathbf{M}_2, \cdots, \mathbf{M}_N\}$

Do
  $\Delta\mathbf{M}_{ij} = \hat{\mathbf{M}}_i \hat{\mathbf{M}}_{ij} \hat{\mathbf{M}}_j^{-1}$;
  $\Delta\mathbf{m}_{ij} = \log(\Delta\mathbf{M}_{ij})$;
  $\Delta\mathrm{v}_{ij} = vec(\Delta\mathbf{m}_{ij})$;
  $\Im = D^{\dagger} V_{ij}$;
  for i=2:N
    $\Delta\mathbf{m}_i = rvec(\Delta v_i)$;
    $\mathbf{M}_i = \exp(\Delta\mathbf{m}_i)\mathbf{M}_i$;
    $\hat{\mathbf{M}}_i = \mathbf{M}_i$;
  end
Until $|\Delta\Im|| < \varepsilon$

Suppose $\mathbf{M}_i(\mathbf{M_j})$ denotes the global motion of the ith (jth) grid map to the reference map, $\mathbf{M}_{ij}$ indicates the relative motion between the ith grid map and the jth grid map. They obey the constraint $\mathbf{M}_{ij} = \mathbf{M}_i{}^{-1}\mathbf{M}_j$. For the problem of multiple map merging, the motions $\mathbf{M}_i$ and $\mathbf{M}_j$ are variables required to be estimated. While, $\mathbf{M}_{ij}$ can be approximated by the one $\hat{\mathbf{M}}_{ij}$ estimated from the pair-wise map merging. In other words, $\mathbf{M}_{ij}$ and $\hat{\mathbf{M}}_{ij}$ is very approximate. Therefore:

$$\Delta\mathbf{m}_{ij} = \mathrm{logm}(\mathbf{M}_i \hat{\mathbf{M}}_{ij} \mathbf{M}_j{}^{-1}) = \Delta\mathbf{m}_j - \Delta\mathbf{m}_i. \tag{15}$$

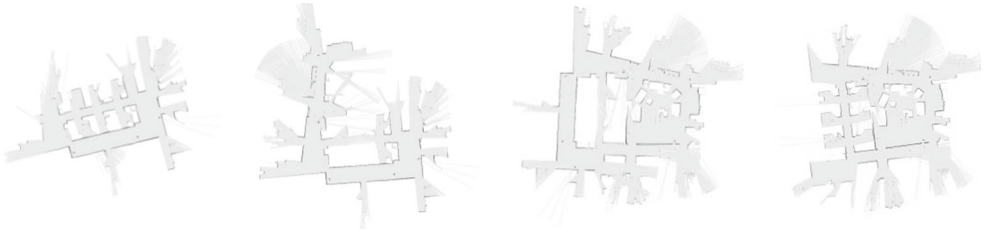

Fig. 5 Grid maps built from Tim.log, which is divided into four parts

As the column vector v represents another form of $\mathbf{m}$, the same relationship also holds for the column vector, i.e. $\Delta v_{ij} = \Delta v_j - \Delta v_i$. Obviously, all the column vectors $\{\Delta v_i\}_{i=1}^{N}$ can be concatenated into one large vector $\Im = [v_1; v_2; \cdots; v_N]$. Subsequently, the equation $\Delta v_{ij} = \Delta v_j - \Delta v_i$ can be transformed into the following form:

$$\Delta v_{ij} = \mathbf{D}_{ij}\Im = [\cdots, \mathbf{I}_3, \cdots, -\mathbf{I}_3]\Im \tag{16}$$

where $\mathbf{I}_3$ is the 3D identity matrix, $\mathbf{D}_{ij}$ can be viewed as an indicator matrices of size $3 \times (3N-3)$ with matrices $\mathbf{I}_3$ and $-\mathbf{I}_3$ at position j and i, respectively. As there are a set of reliable relative motions confirmed by the optimal MCS, it is convenient to concatenate all increment vectors of relative motions into one large vector $\mathbf{V} = \left[\Delta v_{ij_1};\ \Delta v_{ij2};\ \ldots\right]$, Similarly, all the indicator matrices can also be concatenated into one large matrix $\mathbf{D} = \left[\mathbf{D}_{ij_1};\ \mathbf{D}_{ij2};\ \ldots\right]$. According to Eq. 16, there exists the following relationships:

$$\mathbf{V} = \mathbf{D}\Im \tag{17}$$

and

$$\Im = \mathbf{D}^{\dagger}\mathbf{V}, \tag{18}$$

where $\mathbf{D}^{\dagger}$ denotes the pseudo inverse matrix of $\mathbf{D}$. Given the initial global motion $\{\hat{\mathbf{M}}_i\}_{i=1}^{N}$, the increment vectors $\{\Delta v_i\}_{i=1}^{N}$ can be incorporated to refine the global motion as follows:

$$\mathbf{M}_i = \text{expm}(\text{rvec}(\Delta \mathbf{v}_i))\,\hat{\mathbf{M}}_i \quad (i = 2, 3, ..., N) \tag{19}$$

where the function $expm(.)$ denotes the exponential operation of matrix. As displayed in Eq. 14, the motion averaging algorithm cannot obtain the closed-form solution for global motions, so it is required to repeat the refinement until some stop conditions are satisfied. The sketch of the global motion refining algorithm is shown in Algorithm 3.

After motion averaging, accurate global motions can be obtained for merging multiple grid maps.

3.4 Implementation

As the global motions have been estimated, it is easy to integrate all local grid maps into a single global map. In our previous work, we proposed an pair-wise map fusion method [18], which can be repeatedly utilized to fuse two local maps until all local grid maps are fused into one global map.

Given a set of unordered grid maps, the proposed approach can achieve multiple grid map merging as follows: (1) Extract the SIFT features and edge point sets from all grid maps; (2) Estimate the relative motions for many map pairs by Algorithm 1; (3) Obtain the initial global motions and reliable relative motions by the Algorithm 2; (4) Acquire the fine global motions by the Algorithm 3; (5) Fuse all grid maps based on the fine global motions.

4 Experimental Results

To verify the performance of the proposed approach, a set of experiments were tested on four public datasets: Tim.log,[1] Loop25.log,[2] Intel.log and Fr079.log,[3] which were recorded by mobile robots equipped with a laser range finder and odometer. To simulate multi-robot systems, they can be separated into four, four, eight and eleven parts, respectively. By applying the SLAM algorithm [31], they can be used to build local grid map sets for testing the proposed approach. These grid map sets are displayed in Figs. 5, 6, 7 and 8, respectively. Experiments were implemented in MATLAB on a four-core 3.6GHz computer with 8GB of memory.

4.1 Validation

To validate the proposed approach, it was firstly tested on the grid map set built from Fr079.log. As shown in Fig. 8, there are eleven unordered grid maps, which require to be merged. For the convenience of analysis, the method in [32] was introduced to estimate the overlap percentage of each map pair. Figure 9a shows the estimated overlap percentage of each map pair. During pair-wise merging, true feature matches can be detected between each grid map pairs. Figure 9d displays the detected number of true feature matches for all grid map pairs. As shown in Fig. 9d, there are a portion of map pairs, which are lack of enough true feature

[1] http://www-personal.acfr.usyd.edu.au/tbailey/software/scan_matching.zip

[2] http://www.cs.duke.edu/~parr/dpslam/

[3] http://www.ipb.uni-bonn.de/index.php/data/

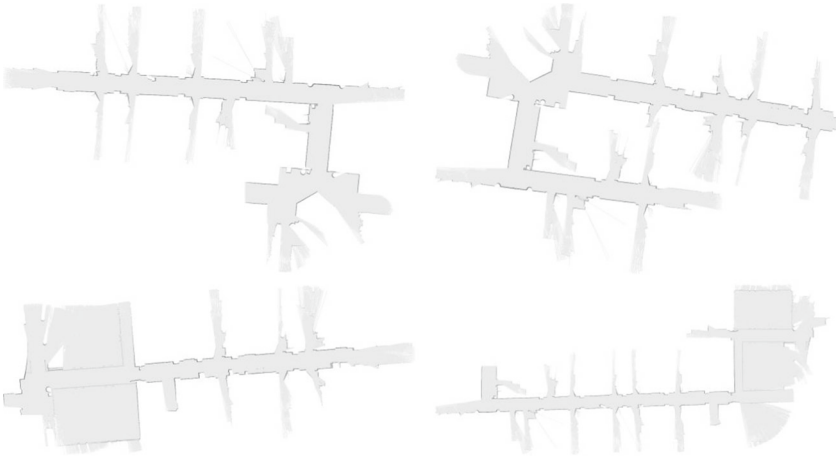

Fig. 6 Grid maps built from Loop25.log, which is divided into four parts

Fig. 7 Grid maps built from Intel.log, which is divided into eight parts

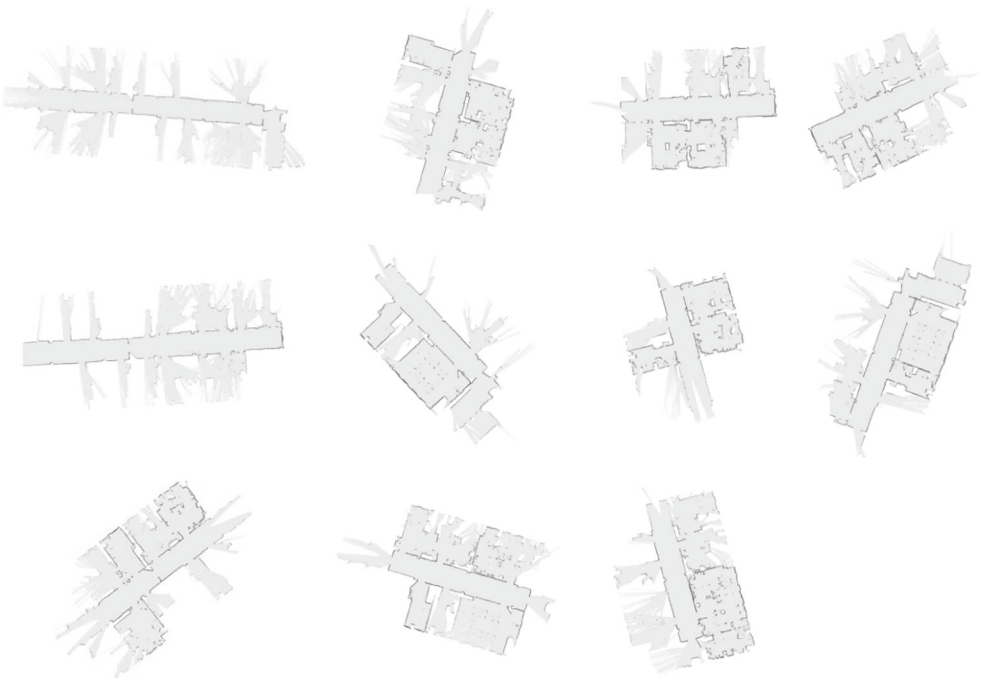

Fig. 8 Grid maps built from Fr079.log, which is divided into eleven parts

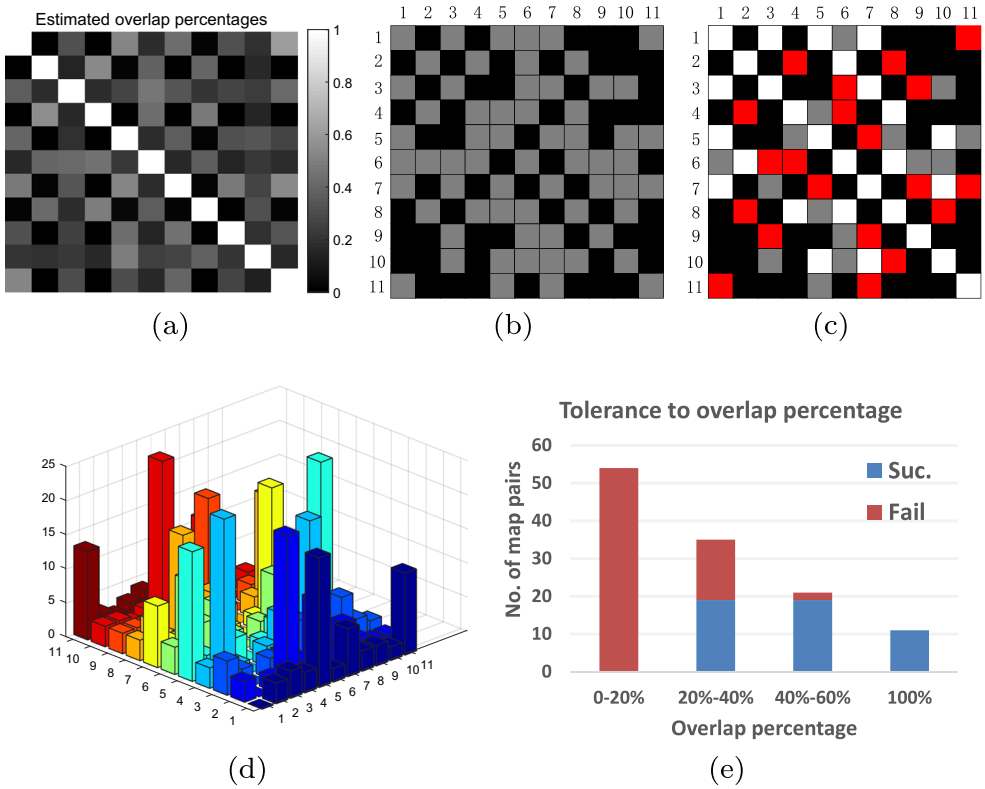

Fig. 9 Intermediate results of the proposed approach. **a** The estimated overlap percentage of each map pair. **b** Map pairs containing estimated relative motions are denoted in gray. **c** The relative motions of the optimal MCS are denoted in the red, other reliable relative motions are denoted in the white and unreliable relative motions are denoted in the gray. **d** The number of detected true feature matches of each map pairs. **e** The tolerance of pair-wise merging method to overlap percentages

matches due to the low overlap percentages or even non-overlapping. For these map pairs, it is difficult to estimate their relative motions. To analyze the limitation of the pair-wise merging, we tested its tolerance to overlap percentages. More specifically, we used the pair-wise merging method to merge each map pair in Fr079.log and recorded the registration results of all these map pairs with respect to the overlap percentages in Fig. 9e. As shown in Fig. 9e, good pair-wise registration results can be obtained when the overlap percentages of map pairs are larger than 40%. In the range [20%,40%], there are almost half of map pairs, whose relative motions can be successfully estimated. However, we haven't come up a way to align those map pairs, whose overlap percentages are less than 20%. For efficiency, the proposed approach only applies the pair-wise merging method to these map pairs, which at least contains four detected true feature matches. Given the true feature matches, initial relative motions can be provided to the TrICP algorithm so as to refine the relative motions for grid map pairs. Figure 9b indicates these map pairs, which can obtain their estimated relative motions. Due to some reasons, the pair-wise merging method may obtain some unreliable relative motions.

Subsequently, the undirected graph should be constructed based on all grid maps and estimated relative motions. On the constructed graph, it is easy to randomly sample the MCS, which contains $(N-1)$ estimated relative motions. As the number of estimated relative motions are more than $(N-1)$, the residual relative motions can be utilized to confirm whether the randomly sampled MCS is the optimal one or not. The process of sampling and confirming MCS should be repeated until the preset iteration number reaches. As a result, the optimal MCS can be searched out with all the reliable relative motions. Figure 9c displays all reliable relative motions and $(N-1)$ relative motions involved in the optimal MCS. As shown in Fig. 9c, there are some of

Fig. 10 The demonstration of one unreliable relative motion, which is estimated by the pair-wise merging method. **a** Model map. **b** Subject map. **c** Merging result based on initial relative motions. **d** Merging result based on estimated relative motions

Fig. 11 The merging of multiple grid maps based different global motions. **a** Global motions estimated from the relative motions involved in the optimal MCS. **b** Global motions estimated from all reliable motions

map pairs, whose estimated relative motions are unreliable. These unreliable relative motions may be caused by two reasons: (1) False true feature matches can only provide invalid initial relative motions to the TrICP algorithm. (2) Even given moderate initial relative motions, the TrICP algorithm may be trapped into local minimum due to the property of local convergence. To view them in a more intuitive way, Fig. 10 displays the merging results of one map pair, which is denoted in the gray in Fig. 9c. As shown in Fig. 10, the relative motion of this map pair is really unexpected, so it should be eliminated by the optimal MCS.

As the optimal MCS contains the minimum set of good relative motions, they can be employed to estimate initial global motions. Figure 11a shows the multiple map merging results based on the initial global motions. As shown in Fig. 11a, the initial global motions are not so satisfactory due to the accumulative errors. Hence, they should further be refined by the motion averaging algorithm. Given all reliable relative motions, the motion averaging algorithm can be utilized to calculate accurate global motions for the merging of multiple grid maps. Figure 11b illustrates the final merging result of multiple grid maps. As shown in Fig. 11, it is really necessary to apply the motion averaging algorithm, which can result in good merging results.

In one word, the proposed approach can accomplish the simultaneous merging of multiple grid maps with good accuracy.

4.2 Comparison

As mentioned above, there are four modules in the proposed approach: pair-wise grid map merging, MCS sampling and confirming, motion averaging as well as grid map fusion, which are abbreviated as PW, MCS, MA and FUSE, respectively. Before the comparison with other approaches, the proposed approach was tested on four datasets so as to illustrate the runtime of each module. To eliminate the randomness, 10 Monte Carlo (MC) trials were conducted on each dataset and the mean runtime of four modules are reported in Table 1. As shown in Table 1, the PW is the most time-consuming module in the proposed approach. Besides, the runtime of FUSE is almost proportional to the number of local grid maps to be merged.

To illustrate its superiority, the proposed approach requires to be compared with other related grid map merging approaches. However, to the best of our knowledge, few approaches can really accomplish the simultaneous merging of multiple grid maps. Therefore, the proposed approach is compared with three combined approaches: the sequential merging approach, which is based on the pair-wise merging algorithm presented in [16], PW+MA and PW+MCS. Experiments were tested on four grid map sets, which are displayed in Figs. 5, 6, 7 and 8, respectively. To eliminate the randomness, 10 Monte Carlo (MC) trials were conducted for all datasets. As there is no ground truth of global motions, the error criterion presented in [20] can be utilized to quantitatively analyze the accuracy of completed merging approaches. During experiments, the average of merging error, the standard deviation of merging error and the mean runtime were recorded in Table 2. To view the results in a more intuitive way, Fig. 12 shows the merging results of three data sets for these completed approaches. As shown in Table 2 and Fig. 12, the proposed approach can obtain more efficient and accurate merging results than that of the sequential merging approach.

To merge multiple grid maps, the sequential merging approach estimate the relative motion of two grid maps and integrate them into one grid map, which will further be merged with another new grid map. The process of estimation and merging is repeated until all local grid maps are integrated into one global grid map. Although this approach is straight-forward, it suffers from the well-known problem that merging errors accumulate at each step. As the grid map grows, the accumulate errors may lead to the failure of map merging. Therefore, the sequential merging approach can not always accomplish the merging

Table 1 The mean runtime (s) of each module in the proposed approach

Dataset	Tim	Intel	Loop25	Fr079
PW	4.4378	18.0656	10.4682	17.7097
MCS	0.0397	0.0833	0.0739	0.1596
MA	0.3568	1.3674	0.2189	1.5914
FUSE	1.1337	4.7781	2.3044	5.7882

Table 2 Performance comparison for map merging of grid maps

Dataset			SeqM [16]	PW+MA	PW+MCS	Our method
	Obj.	Mean	7.5585	0.6086	0.5757	0.5514
Tim		Std	4.0283	0.0613	0.0068	0.0041
	T(s)	Mean	10.1826	5.7437	5.5341	5.8669
	Obj.	Mean	16.9243	28.4815	0.4812	0.4525
Intel		Std	3.0431	25.08537	0.0325	0.0132
	T(s)	Mean	33.3151	24.1164	23.9316	25.2065
	Obj.	Mean	4.7887	1.1665	0.5873	0.5642
Loop25		Std	1.7176	0.5216	0.0053	0.0021
	T(s)	Mean	31.8735	12.8843	12.9101	13.0508
	Obj.	Mean	5.9350	4.0252	0.3079	0.2919
Fr079		Std	5.0454	4.9186	0.0044	0.0029
	T(s)	Mean	34.9208	23.5246	23.3295	25.1500

of multiple grid maps. What's more, this approach requires to repeatedly extract SIFT features from the new merged grid map, so it is less efficient. Meanwhile, as shown in Table 2 and Fig. 12, the PW+MA approach can not always work well for all datasets. This is because the pair-wise merging method may obtain unreliable relative motions. Without the MCS module, the application of MA on all relative motions can lead to the failure of multiple grid map merging. Therefore, the MCS module is required. Although the PW+MCS approach can obtain acceptable merging results, it is not accurate enough. This is because this approach only utilizes the minimum set of reliable relative motions to estimate the global motions. Hence, more reliable relative motions are required to obtain good merging results by the MA algorithm.

Different from those combined approaches, the proposed approach utilizes the pair-wise merging approach to estimate relative motions of several map pairs. Among these estimated relative motions, there may exist unreliable ones. Subsequently, it randomly samples a minimum set of relative motions to estimate the initial global motions, which can be further confirmed by all relative motions. By repeating the process of sampling and confirming, it can find the optimal MCS for the estimation of initial

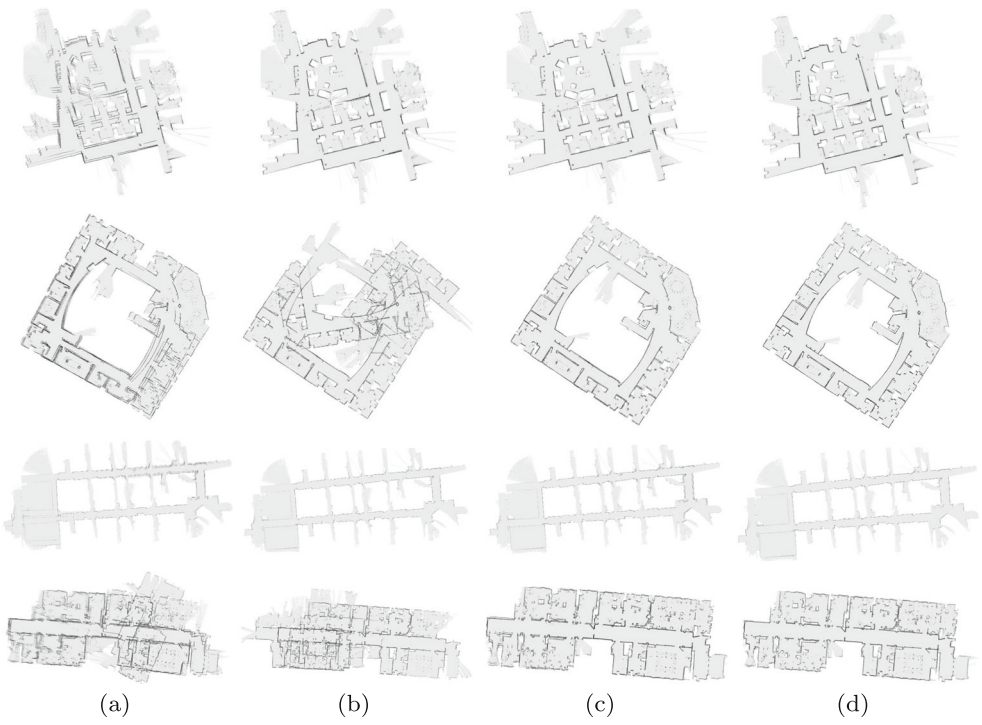

Fig. 12 Multiple grid map merging results of four data sets for four competed approaches. **a** Sequential merging Results. **b** PW+MA **c** PW+MCS **d** Our Results

Table 3 Map merging results for the grid maps with different orders

Dataset	ID	Error		T(s)	Suc.
		(Coarse)	(Fine)		
Tim	Order1	0.5713	0.5546	6.2307	Y
	Order2	0.5715	0.5560	5.7976	Y
	Order3	0.5713	0.5576	6.0282	Y
	Order4	0.5874	0.5497	5.5812	Y
Intel	Order1	0.4877	0.4509	25.2479	Y
	Order2	0.4906	0.4470	24.9545	Y
	Order3	0.4882	0.4390	25.8127	Y
	Order4	0.4944	0.4560	24.7972	Y
Loop25	Order1	0.5881	0.5645	12.8814	Y
	Order2	0.5876	0.5641	12.8446	Y
	Order3	0.5873	0.5638	12.8176	Y
	Order4	0.5991	0.5640	12.9122	Y
Fr079	Order1	0.3083	0.2940	25.7781	Y
	Order2	0.3110	0.2938	26.2362	Y
	Order3	0.3084	0.2933	26.7617	Y
	Order4	0.3042	0.2936	24.9469	Y

global motions and confirm all reliable relative motions. Given the initial global motions, the MA algorithm can be applied to all reliable relative motions so as to calculate the accurate global motions for simultaneous merging of

Fig. 13 Merged maps of Tim.log, Intel.log and Loop25.log. **a** Merged maps based on initial global motions. **b** Merged maps based on the refined global motions

multiple grid maps. Hence, the proposed approach can always accomplish merging multiple grid maps with good efficiency and accuracy.

4.3 Robustness to Grid Map Orders

To verify its robustness, the proposed approach was tested on four data sets with different group of orders, which can be randomly changed. During the experiment, grid maps with different orders were viewed as inputs and four groups of map merging results for each data set were recorded in Table 3. To view the results in a more intuitive way, Fig. 13 displays the merged maps for Tim.log, Loop25.log and Intel.log under one group of grid map order. As shown in Table 3, the running time of the proposed approach is varied due to the size of grid map set. Besides, for each data set, the proposed approach can obtain almost the same merging results for different map orders.

Before performing multiple gird merging, an exhaustive search strategy is utilized to independently estimate the relative motions of map pairs, and the results can be utilized to construct a undirected graph with all grid maps. On this constructed graph, a set of MCS are randomly sampled and then confirmed by all other relative motions. Subsequently, no matter what the order of grid maps is, the proposed approach can always search for the optimal MCS and obtain all the reliable relative motions. Based on the optimal MCS, it is easy to estimate good initial global motions. As shown in Fig. 13, initial global motions are not very satisfactory, so they can further be refined by the MA algorithm with all the reliable relative motions. As shown in Tables 1 and 3, the MA only costs a small portion of merging time but can seriously reduce the merging error. Accordingly, the proposed approach can always obtain the grid map merging results, which are independent with the order of grid maps to be merged. Therefore, the proposed approach is robust to the order of grid maps to be merged.

5 Conclusion

This paper proposes an effective approach for simultaneous merging grid maps built by multiple robots. It first utilizes the pair-wise map merging method to estimate the relative motion of map pairs. For the reason of low overlapping percentage, it may get unreliable relative motions for some map pairs. Therefore, the minimum set of reliable relative motions should be sampled and confirmed by other relative motions so as to eliminate unreliable relative motions. Then, the initial global motions can be estimated from the minimum set of reliable relative motions. Since the unreliable relative motions have been discarded, the motion averaging algorithm can be applied to all reliable relative motions so as to get accurate global motions for map merging. The proposed approach has been tested on the real robot data sets. Experimental results illustrate that the proposed approach can accomplish simultaneous merging multiple maps with good accuracy, efficiency and robustness.

The proposed approach includes some limitations. If one grid map has low overlap percentages with all other grid maps, there is no way to integrate it into the global grid maps. However, most merging approaches proposed so far share this limitations as well. Besides, the proposed approach can not simultaneously merge grid maps in different resolutions. Our future work will focus on addressing the second limitation.

Acknowledgments This work is supported by the National Natural Science Foundation of China under Grant nos. 61573273 and 91648121, the Natural Science Foundation of Shaanxi Province of China under Grant no. 2015JM6301, the Fundamental Research Funds for Central Universities under Grant No. xjj2018214.

References

1. Smith, R., Self, M., Cheeseman, P.: A stochastic map for uncertain spatial relationships. Int. Symp. Robot. Res., 467–474 (1988)
2. Wen, L.D.L., Jarvis, R.: A pure vision-based topological SLAM system. Int. J. Robot. Res. **31**(4), 403–428 (2012)
3. Alitappeh, R.J., Pereira, G.A.S., Arajo, A.R., et al.: Multi-robot deployment using topological maps. J. Intell. Robot. Syst. **86**(3–4), 641–661 (2017)
4. Collins, T.: Occupancy grid learning using contextual forward modelling. J. Intell. Robot. Syst. **64**(3–4), 505–542 (2011)
5. Carlone, L., Ng, M.K., Du, J., et al.: Simultaneous localization and mapping using rao-blackwellized particle filters in multi robot systems. J. Intell. Robot. Syst. **63**(2), 283–307 (2011)
6. Choudhary, S., Carlone, L., Nieto, C., et al.: Multi robot object-based SLAM. Int. Symp. Exper. Robot., 729–741 (2016)
7. Lazaro, M.T., Paz, L.M., Pinies, P., et al.: Multi-robot SLAM using condensed measurements. IEEE/RSJ Int. Conf. Intell. Robot. Syst. (IROS) **40**(6), 1069–1076 (2013)
8. Saeedi, S., Trentini, M., Seto, M., et al.: Multiple-robot simultaneous localization and mapping: A review. J. Field Robot. **33**(1), 3–46 (2016)
9. Carpin, S., Birk, A., Jucikas, V.: On map merging. Robot. Auton. Syst. **53**(1), 1–14 (2005)
10. Birk, A., Carpin, S.: Merging occupancy grid maps from multiple robots. Proc. IEEE **94**(7), 1384–1397 (2006)
11. Li, H., Tsukada, M., Nashashibi, F., Parent, M.: Multivehicle cooperative local mapping: a methodology based on occupancy grid map merging. IEEE Trans. Intell. Transp. Syst. **15**(5), 2089–2100 (2014)
12. Carpin, S.: Fast and accurate map merging for multi-robot systems. Auton. Robot. **25**(3), 305–316 (2008)
13. Zhu, J., Du, S., Ma, L., et al.: Merging grid maps via point set registration. Int. J. Robot. Autom. **28**(2), 180–191 (2013)

14. Chetverikov, D., Stepanov, D., Krsek, P.: Robust Euclidean alignment of 3D point sets: the trimmed iterative closest point algorithm. Image Vis. Comput. **23**(3), 299–309 (2005)
15. Phillips, J.M., Liu, R., Tomasi, C.: Outlier robust ICP for minimizing fractional RMSD. In: Sixth International Conference on 3-D Digital Imaging and Modeling, pp. 427–434 (2007)
16. Blanco, J.L., Gonzlezjimnez, J., Fernndezmadrigal, J.A.: A robust, multi-hypothesis approach to matching occupancy grid maps. Robotica **31**(5), 687–701 (2013)
17. Saeedi, S., Paull, L., Trentini, M., et al.: Map merging for multiple robots using Hough peak matching. Robot. Auton. Syst. **62**(10), 1408–1424 (2014)
18. Ma, L., Zhu, J., Zhu, L., et al.: Merging grid maps of different resolutions by scaling registration. Robotica **34**(11), 2516–2531 (2016)
19. Lei, H., Jiang, G., Quan, L.: Fast descriptors and correspondence propagation for robust global point cloud registration. IEEE Trans. Image Process. **26**(8), 3614–3623 (2017)
20. Zhu, J., Zhu, L., Li, Z.: Automatic multi-view registration of unordered range scans without feature extraction. Neurocomputing **171**(C), 1444–1453 (2016)
21. Evangelidis, G.D., Kounades-Bastian, D., Horaud, R., Psarakis, E.Z.: A generative model for the joint registration of multiple point sets. Proc. European Conf. Comput. Vis. (ECCV) **8695**, 109–122 (2014)
22. Govindu, V.M., Pooja, A.: On averaging multiview relations for 3D scan registration. IEEE Trans. Image Process. **23**(3), 1289–1302 (2014)
23. Zhu, J.: Surface reconstruction via efficient and accurate registration of multiview range scans. Opt. Eng. **53**(10), 102104 (2014)
24. Arrigoni, F., Rossi, B., Fusiello, A.: Global registration of 3D point sets via LRS decomposition. In: Proceedings of European Conference on Computer Vision (ECCV), pp. 489–501 (2016)
25. Zhu, J., Zhu, L., Jiang, Z., et al.: Local to global registration of multi-view range scans using spanning tree. Comput. Electr. Eng. **58**, 477–488 (2017)
26. Govindu, V.M.: Lie-algebraic averaging for globally consistent motion estimation. Comput. Vis. Pattern Recogn. (CVPR) **1**, I-684-I-691 (2004)
27. Govindu, V.M.: Robustness in motion averaging. Asian Conf. Comput. Vis. **3852**, 457–466 (2006)
28. Zhu, J., Meng, D., Li, Z.: Robust registration of partially overlapping point sets via genetic algorithm with growth operator. IET Image Process. **8**(10), 582–590 (2014)
29. Lowe, D.G.: Distinctive image features from scale-invariant keypoints. Int. J. Comput. Vis. **60**(2), 91–110 (2004)
30. Brown, M.L. et al.: Automatic panoramic image stitching using invariant features. Int. J. Comput. Vision **74**(1), 59–73 (2007)
31. Eliazar, A.I., Parr, R.: Hierarchical linear/constant time SLAM using particle filters for dense maps, NIPS, 339–346 (2005)
32. Li, Z., Zhu, J., Lan, K., et al.: Improved techniques for multi-view registration with motion averaging. In: International Conference on 3d Vision, pp. 713–719 (2014)

Zutao Jiang received his B.S. degree from software engineering,Central South University, in 2015. He is currently a doctoral candidate of Xi'an Jiaotong University. His research interests include computer vision and machine learning.

Jihua Zhu received his Ph.D. degree in pattern recognition and intelligence system from Xi'an Jiaotong University, China, in 2011. He is an Associate Professor in the School of Software Engineering at Xi'an Jiaotong University. His research interests include mobile robot and computer vision.

Yaochen Li received the B.E. degree in computer science and Ph.D. degree in control science and engineering from Xi'an Jiaotong University, China in 2008 and 2016, respectively. He is currently an assistant professor in School of Software Engineering, Xi'an Jiaotong University. His research interests include image processing and analysis, computer vision and intelligent systems.

Jun Wang (M'2014) received his Ph.D. degree in pattern recognition and intelligence systems from the School of Computer Science and Technology in Nanjing University of Science and Technology, Nanjing (NUST), China, in 2011. He is currently an Associate Professor with the School of Digital Media, Jiangnan University, China. He has published more than 40 articles in international/national journals. His research interests include machine learning and computer vision.

Zhongyu Li is a Ph.D. student in the Department of Computer Science at the University of North Carolina at Charlotte. He received his B.E. and M.E. degree from Xi'an Jiaotong University in 2012 and 2015 respectively. His research focuses on computer vision, machine learning and medical image analysis.

Huimin Lu received M.S. degrees in Electrical Engineering from Kyushu Institute of Technology and Yangzhou University in 2011. He received a Ph.D. degree in Electrical Engineering from Kyushu Institute of Technology in 2014. From 2013 to 2016, he was a JSPS research fellow at Kyushu Institute of Technology, Japan. Currently, he is an Assistant Professor in Kyushu Institute of Technology and an Excellent Young Researcher of MEXT-Japan. His research interests including computer vision, robotics, artificial intelligence and ocean observing.